Low-coherence enhanced backscattering beyond diffusion

Min Xu

Department of Physics, Fairfield University, 1073 North Benson Road, Fairfield, Connecticut 06824, USA
mxu@mail.fairfield.edu

Received January 11, 2008; revised April 6, 2008; accepted April 28, 2008;
posted May 1, 2008 (Doc. ID 91425); published May 29, 2008

An analytical theory for coherent backscattering (CBS) of low-coherence light is presented. An expression linking the CBS profile to the radial distribution of the incoherent backscattered light is derived when the incident light is partially spatially coherent. The backscattered snake light, which has experienced exactly two large-angle scatterings, is taken into account together with the diffuse light in the analysis. Monte Carlo simulations demonstrate that the model describes well the CBS profile as long as the spatial coherence length, L_c, of the incident beam is larger than the scattering mean free path of light in the medium. The intensity of the enhanced backscattered light in the exact backscattering direction and the width of the CBS cone are found to be proportional to L_c and L_c^{-1}, respectively, in the limit of small L_c. © 2008 Optical Society of America

OCIS codes: 030.1670, 290.1350, 290.4210, 290.7050, 170.4580.

Coherent backscattering (CBS) is one intriguing phenomenon of multiple scattering light where the backscattered light is found to be enhanced around the exact backscattering direction, originating from the constructive interference between the light waves propagating along a pair of time-reversal trajectories [1,2]. For an incident coherent beam, the CBS peak is enhanced up to two times in the exact backscattering direction, and the width of the CBS cone is proportional to λ/l_t, the ratio of the wavelength and the transport mean free path of light in the medium [3]. It was observed in 1991 that the CBS cone can be much wider with a significantly reduced peak and suppressed speckle when illuminated by a low-coherence source with the spatial coherent length $L_c < l_t$ [4]. In this case, only light remitting within the coherence area $\sim L_c^2$, much smaller than the illuminated area, participates in enhanced backscattering. Diffuse light, which travels much deeper into the medium, is greatly rejected. This is of particular interest for biomedical imaging [5] owing to the potential to restrict the probing of light to the superficial layer of tissue where most cancers initiate. In this Letter, we will present a simple theory for low-coherence enhanced backscattering (LEBS) of scalar light. First, a correct expression [Eq. (4)] linking the CBS profile to the radial profile of the incoherent backscattered light is derived. Second, LEBS is shown to be well modeled by the theory taking into account both "snake" and diffuse light as long as L_c is larger than the scattering mean free path, l_s. The theory predicts that the intensity of the enhanced backscattered light in the exact backscattering direction and the width of the CBS cone are proportional to L_c/l_t and λ/L_c, respectively, when $L_c \ll l_t$, agreeing with both Monte Carlo (MC) and reported experimental observations [5].

A pair of time-reversal trajectories are displayed in Fig. 1. When illuminated by a collimated low-coherence beam with near normal incidence, the intensity of LEBS light is expressed as [3]

$$I_{\mathrm{CBS}}(\mathbf{q}_\perp) = \frac{1}{A}\int \mathrm{d}\boldsymbol{\rho}_1 \int \mathrm{d}\boldsymbol{\rho}_2 I(\boldsymbol{\rho}_2 - \boldsymbol{\rho}_1) \times \exp[i\mathbf{q}_\perp \cdot (\boldsymbol{\rho}_2 - \boldsymbol{\rho}_1)] J(\boldsymbol{\rho}_1, \boldsymbol{\rho}_2). \quad (1)$$

Here, $\boldsymbol{\rho}_{1,2}$ are the projections on the sample surface ($z=0$) of vectors connecting the center of the source to $P_{1,2}$, respectively; the integrations of $\boldsymbol{\rho}_{1,2}$ are over the illumination area $A=\pi b^2$ of radius b; $\mathbf{q}_\perp = k(\mathbf{s}_i + \mathbf{s}_f)$; and $q_\perp \simeq k\theta_b$, where $k=2\pi/\lambda$ is the wavenumber of light in the air and θ_b is the angle between the incident and outgoing directions. $I(\boldsymbol{\rho})$ is the intensity of incoherent backscattered light for a beam incident upon the medium in s_i at the origin and escaping the medium in s_f at $\boldsymbol{\rho}$. $J(\boldsymbol{\rho}_1, \boldsymbol{\rho}_2)$ is the complex degree of coherence of fields $V_{1,2}$ at $P_{1,2}$, given by [9]

$$J(\boldsymbol{\rho}_1, \boldsymbol{\rho}_2) = \langle V_1^* V_2 \rangle = 2\frac{J_1(|\boldsymbol{\rho}_1 - \boldsymbol{\rho}_2|/L_c)}{|\boldsymbol{\rho}_1 - \boldsymbol{\rho}_2|/L_c} \exp\left(i\frac{\rho_2^2 - \rho_1^2}{2aL_c}\right), \quad (2)$$

for a partially coherent circular uniform source of radius a and with a spatial coherence length L_c on the $z=0$ plane.

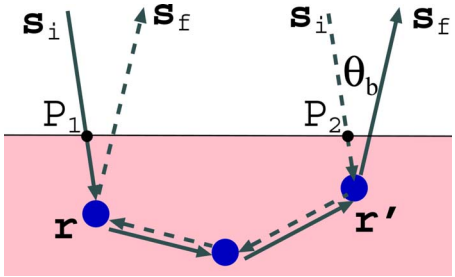

Fig. 1. (Color online) Pair of time-reversal trajectories (solid and dashed lines) for a beam incident in the $\mathbf{s}_i$ direction and escaping in the $\mathbf{s}_f$ direction. A low-coherent source introduces an additional phase correlation between the light fields at the illumination points P_1 and P_2.

By replacing the integration over $\boldsymbol{\rho}_2$ to $\boldsymbol{\rho}=\boldsymbol{\rho}_2-\boldsymbol{\rho}_1$, the integration over $\boldsymbol{\rho}_1$ in Eq. (1) can be performed to obtain

$$I_{\mathrm{CBS}}(\mathbf{q}) = \int \mathrm{d}\boldsymbol{\rho} I(\boldsymbol{\rho}) \exp(i\mathbf{q}_\perp \cdot \boldsymbol{\rho}) \gamma(\rho) \exp\left(i\frac{\rho^2}{2aL_c}\right) \times \left[2\frac{J_1(\rho/L_c)}{\rho/L_c}\right]^2, \quad (3)$$

where $\gamma(\rho)=(2/\pi)[\arccos(\rho/2b)-(\rho/2b)\sqrt{1-(\rho^2/4b^2)}]$ is the characteristic function of a uniform disk. The integration of $\boldsymbol{\rho}$ is over a disk of radius $2b$. Accounting for the fact that appreciable nonzero values of the integrand in Eq. (3) come from $\rho<3L_c$, Eq. (3) reduces to

$$I_{\mathrm{CBS}}(\mathbf{q}_\perp) = 2\pi \int_0^{+\infty} \rho \mathrm{d}\rho I(\rho) J_0(q_\perp \rho) \left[2\frac{J_1(\rho/L_c)}{\rho/L_c}\right]^2, \quad (4)$$

as long as $L_c \ll a,b$ where the integration of $\boldsymbol{\rho}$ is extended to cover the whole $z=0$ plane. The condition $L_c \ll a,b$ holds in most LEBS measurements. The additional factor of $2J_1(\rho/L_c)/(\rho/L_c)$ in Eq. (4) originates from the phase factor in Eq. (2) and was ignored in earlier publications [7].

The main equation (4) can also be proved by use of the angular correlation description of the illuminating light field. The angular correlation function for the spatially partially coherent source can be obtained by Fourier transform of Eq. (2) [8]. The self-angular correlation function is found to be

$$\mathcal{A}(\mathbf{s},\mathbf{s}) = \frac{k^2}{(2\pi)^2} \int \mathrm{d}\boldsymbol{\rho} \left[2\frac{J_1(\rho/L_c)}{\rho/L_c}\right]^2 \exp[-ik(\mathbf{s}-\mathbf{s}_0)\cdot\boldsymbol{\rho}], \quad (5)$$

normalized to $\int \mathcal{A}(\mathbf{s},\mathbf{s})\mathrm{d}\mathbf{s}=1$, where $\mathbf{s}_0$ is the direction of the optical axis of the incident beam. The divergence of the incident beam is $\sim 1/kL_c$. The intensity of coherent backscattered light is given by the incoherent superposition of light incident upon all directions [9], $\int \mathrm{d}\boldsymbol{\rho} I(\boldsymbol{\rho}) \exp[ik(\mathbf{s}+\mathbf{s}_f)\cdot\boldsymbol{\rho}]\mathcal{A}(\mathbf{s},\mathbf{s})\mathrm{d}\mathbf{s}$, yielding the same answer [Eq. (4)].

The CBS profile I_{CBS} is determined mainly by $I(\rho)$ within the region $\rho<3L_c$. It is expected the details of light scattering inside the turbid medium plays a more pronounced role when L_c is shortened below the scattering mean free path, l_s. On the other hand, the intensity $I(\rho)$ when $\rho \gtrsim l_s$ depends primarily on the transport mean free path, $l_t=l_s/(1-g)$, where g is the mean cosine of scattering angles. In highly forward scattering media, such as tissue, $l_t \gg l_s$.

In the latter case, the focus of this Letter, the photons may be categorized into snake and diffuse light. Assuming near normal incidence and detection, the snake light experiences the first large-angle scattering at $\mathbf{r}=(0,z)$, moves a distance R, then experiences the second large-angle scattering at $\mathbf{r}'=(\boldsymbol{\rho},z')$ before escaping the medium without further large-angle scattering. The diffusive light experiences additional large-angle scattering during its movement between $\mathbf{r}$ and $\mathbf{r}'$. The total intensity is given by

$$I(\rho) = \frac{1}{4\pi l_t^2} \int_0^{+\infty} \mathrm{d}z \int_0^{+\infty} \mathrm{d}z' \exp\left(-\frac{z+z'}{l_t}\right) \times [G^{(\mathrm{snake})}(R) + G^{(\mathrm{diffuse})}(\mathbf{r},\mathbf{r}')], \quad (6)$$

where $R=\sqrt{\rho^2+(z-z')^2}$, $G^{(\mathrm{snake})}(r)=\exp(-r/l_t)/4\pi r^2$, and $G^{(\mathrm{diffuse})}(\mathbf{r},\mathbf{r}')=G_0(\rho,z-z')-G_0(\rho,z+z'+2z_e)$ are the Green's functions inside the semi-infinite medium with $G_0(r)=3/4\pi l_t r$ and z_e is the extrapolation length dependent on the refractive index mismatch at the interface and takes the value of $2l_t/3$ for an index-matched boundary [10]. $G^{(\mathrm{snake})}(r)$ is the ballistic propagator for an isotropic source inside an isotropically scattering turbid medium.

Equations (4) and (6) provide a complete solution to low-coherence backscattering for scalar light. In the limit of $L_c \ll l_t$, the CBS peak $I_{\mathrm{CBS}}(0)=(3\pi)^{-1}L_c/l_t$ and the FWHM $2\theta_{1/2} \equiv 2k^{-1}q_{1/2}$ with $q_{1/2}=1.42/L_c$. Such a behavior is the result of $I(\rho) \propto 1/\rho$ when $\rho \to 0$. In the limit of $L_c \gg l_t$, the incorporation of the snake light improves the fitting to the experimental CBS cone more than the diffuse light alone [6], and the CBS peak and width approaches $(3/8\pi)(1+2z_e/l_t+1/3\ \ln 2)$ and $q_{1/2}=1/3l_t$, respectively. The baseline intensity of incoherent backscattering light is given by $I_{\mathrm{base}}=\int \mathrm{d}\boldsymbol{\rho} I(\rho)=(3/8\pi)(1+2z_e/l_t+1/3\ \ln 2)$.

Electric field MC simulations were performed for low-coherence backscattering of light from a semi-infinite medium of water solutions of Rayleigh and Mie scatterers [11,12]. The Mie scatterers are polystyrene spheres of diameter 1.5 μm and an anisotropy factor $g=0.92$ at the wavelength, 0.515 μm, of the incident beam. In simulation a matched refractive index boundary is assumed. The backscattered light intensity $I(\rho)$ in the exact backscattering direction at a distance ρ away from the incidence point is simulated for a pencil beam normally incident upon the surface.

Figure 2 shows the profiles of $I(\rho)$ for Rayleigh and Mie scatterers and the comparison to the theory

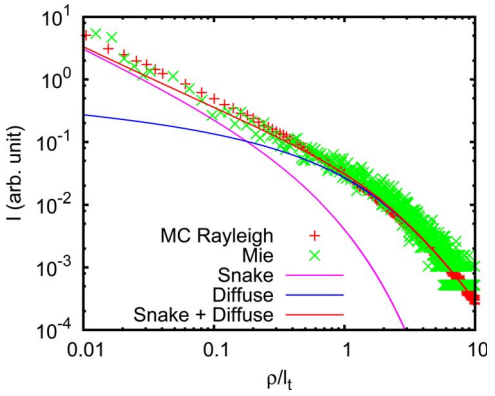

Fig. 2. (Color online) Profiles of the backscattered incoherent light intensity $I(\rho)$ versus the normalized radial distance ρ/l_t from MC simulations compared with theoretical predictions for Rayleigh and Mie scatterers ($g=0.92$).

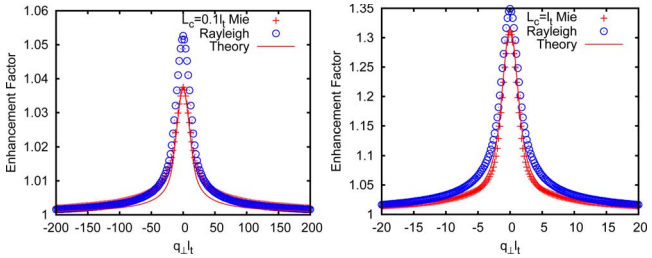

Fig. 3. (Color online) CBS profiles obtained from Monte Carlo simulations compared to the theoretical predictions for Rayleigh and Mie scatterers at $L_c/l_t=0.1$ (left) and 1 (right). The enhancement factor is underestimated by the theory for the Rayleigh scatterer with $L_c=0.1l_t$ as $L_c=0.1l_s$ is much less than the scattering mean free path.

(snake + diffuse) [Eq. (6)] and each separate component. It is evident that the incorporation of the snake component greatly improves the accuracy of $I(\rho)$ when ρ/l_t is small.

Figure 3 displays the CBS profiles obtained from the theory and the MC results. A good agreement for the CBS peak is reached for Mie scatterers when $L_c \geq 0.1l_t=1.2l_s$ and for Rayleigh scatterers when $L_c \geq l_t=l_s$. This suggests that the proposed theory is valid as long as the spatial coherence length is at least l_s. A better agreement is obtained for the CBS cone above the half-maximum as the error in $I(\rho)$ near the origin mainly affects enhanced backscattering into larger angles. Note l_t is much larger than l_s and $l_s/l_t \simeq 0.03-0.1$ for biological tissue. It should also be emphasized here that there is no fitting or scaling.

Figure 4 displays the normalized intensity, $I_{\mathrm{CBS}}(0)/I_{\mathrm{base}}$, and the normalized inverse width, $(q_{1/2}l_t)^{-1}$, of LEBS versus L_c/l_t. The inclusion of the snake component improves significantly the agreement between the theoretical prediction and the MC results. When $L_c<l_t$, the normalized intensity is dominated by the snake component and is proportional to L_c/l_t as predicted, yet the theory underestimates the value of the prefactor slightly. The width predicted by the theory is in excellent agreement with the MC results. The linear relation $q_{1/2}=1.42/L_c$ or $(q_{1/2}l_t)^{-1}=0.70L_c/l_t$ holds well when $L_c<l_t$. In the limit of $L_c \gg l_t$, $(q_{1/2}l_t)^{-1}$ approaches 3 as predicted by the diffusion model. It is also worth pointing out that the contribution of double-scattering light to the CBS peak from MC simulations is ~65% and ~7% for Rayleigh and Mie scatterers, respectively, at $L_c=0.1l_t$. Light scattering by biological tissue is highly forward peaked; similar to the Mie particle investigated here. Double-scattering light hence plays only a minimal role in LEBS by tissue when $L_c \geq 0.1l_t$.

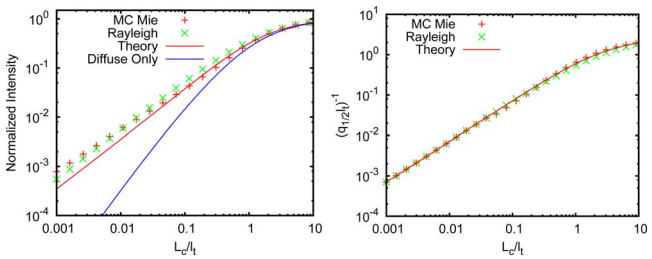

Fig. 4. (Color online) (Left) Normalized intensity $I_{\mathrm{CBS}}(0)/I_{\mathrm{base}}$ and (right) normalized inverse width $(q_{1/2}l_t)^{-1}$ of LEBS versus L_c/l_t.

In conclusion, a simple theory for low-coherence enhanced backscattering (LEBS) of light has been presented. The theory is validated by Monte Carlo simulations of LEBS and reveals the main characteristics of LEBS observed in experiments. The CBS cone—in particular its portion above half-maximum—displays a universal behavior determined solely by the transport mean free path of light in the medium as long as the spatial coherence length of light is larger than the scattering mean free path of light in the medium. The dependence on the details of light scattering in the medium emerges when the spatial coherence length is further shortened below the scattering mean free path. The investigation of the latter case will be reported later.

M. Xu acknowledges the Research Corporation and Fairfield University for their support.

References

1. Y. Kuga and A. Ishimaru, J. Opt. Soc. Am. A **1**, 831 (1984).
2. P.-E. Wolf and G. Maret, Phys. Rev. Lett. **55**, 2696 (1985).
3. E. Akkermans, P. E. Wolf, and R. Maynard, Phys. Rev. Lett. **56**, 1471 (1986).
4. M. Tomita and H. Ikari, Phys. Rev. B **43**, 3716 (1991).
5. Y. L. Kim, Y. Liu, V. M. Turzhitsky, H. K. Roy, R. K. Wali, and V. Backman, Opt. Lett. **29**, 1906 (2004).
6. M. Born and E. Wolf, *Principles of Optics: Electromagnetic Theory of Propagation, Interference and Diffraction of Light*, 7th ed. (Pergamon, 2002), p. 572.
7. Y. L. Kim, V. M. Turzhitsky, Y. Liu, H. K. Roy, R. K. Wali, H. Subramanian, P. Pradhan, and V. Backman, J. Biomed. Opt. **11**, 041125 (2006).
8. E. Wolf, Opt. Lett. **19**, 2024 (1994).
9. T. Okamoto and T. Asakura, Opt. Lett. **21**, 369 (1996).
10. J. X. Zhu, D. J. Pine, and D. A. Weitz, Phys. Rev. A **44**, 3948 (1991).
11. M. Xu, Opt. Express **12**, 6530 (2004).
12. K. G. Phillips, M. Xu, S. K. Gayen, and R. R. Alfano, Opt. Express **13**, 7954 (2005).